



# Three-dimensional cardiac computed tomography compared with autopsied material for the assessment of the mitral valve

Agata Krawczyk-Ożóg<sup>1,2</sup>  | Mateusz K. Hołda<sup>1,3</sup>  | Jakub Batko<sup>1</sup>  |  
Stanisław Bartuś<sup>2,4</sup>  | Renata Rajtar-Salwa<sup>2</sup>

<sup>1</sup>Department of Anatomy, HEART – Heart Embryology and Anatomy Research Team, Jagiellonian University Medical College, Krakow, Poland

<sup>2</sup>Department of Cardiology and Cardiovascular Interventions, University Hospital, Krakow, Poland

<sup>3</sup>Division of Cardiovascular Sciences, The University of Manchester, UK

<sup>4</sup>2<sup>nd</sup> Department of Cardiology, Jagiellonian University Medical College, Kraków, Poland

## Correspondence

Agata Krawczyk-Ożóg, Department of Anatomy, HEART – Heart Embryology and Anatomy Research Team, Jagiellonian University Medical College, 12 Kopernika Street, Kraków 31-034, Poland.  
Email: [agata.krawczyk@uj.edu.pl](mailto:agata.krawczyk@uj.edu.pl)

## Abstract

To compare the morphometrical features of non-diseased mitral valves imaged in three-dimensional (3D) cardiac computed tomography with those analyzed macroscopically in autopsied healthy human hearts. A total of 51 cardiac computed tomography scans and 120 adult autopsied human hearts without cardiovascular disease were examined. The 3D reconstruction and visualization software (Mimics Innovation Suite 22, Materialise) was used for heart chambers semi-automatic segmentation and myocardial manual segmentation to visualize a 3D structure of the mitral valve complex and to perform all measurements. Direct comparison of corresponding mitral valve parameters revealed significant differences between obtained results. Significantly larger intercommisural diameter, aorto-mural diameter, and perimeter of the mitral annulus were observed in tomographic scans (all  $p < 0.0001$ ). However, the intercommisural/aorto-mural diameter ratio showed comparable values for both groups. Nevertheless, the size of anterior mitral leaflet was higher in autopsied material. The height of the P2 scallops was the only parameter that show no significant difference between two groups ( $p = 0.3$ ). The use of 3D postprocessing algorithms provides a very accurate image of the mitral valve structure, which could be useful for the precise non-invasive assessment of mitral valve size and structure. Three-dimensional contrast enhanced cardiac computed tomography significantly overestimates the measurements of the mitral annulus compared to postmortem analysis.

## KEYWORDS

autopsied human heart, computed tomography, image segmentation, mitral annulus, mitral valve

## 1 | INTRODUCTION

The mitral valve apparatus is one of the most complex structures in the human body (Krawczyk-Ożóg, Hołda, Bolechała, et al., 2017; Krawczyk-Ożóg, Hołda, Sorysz, et al., 2017). Mitral regurgitation is a common valvular abnormality worldwide, that affect over two

percent of the total population and has a prevalence that increases with age (Douedi & Douedi, 2021). Standard two-dimensional (2D) transthoracic echocardiography is the first-line imaging method used for the evaluation of mitral valve disorders, but it is often not sufficient to properly visualize the valve and subvalvular apparatus. Complementary to echocardiography examination is contrast-enhanced electrocardiogram-gated cardiac computed tomography. It has several advantages, such as high isotropic spatial resolution, good temporal resolution, a large field of view,

**Abbreviations:** BMI, body mass index; BSA, body surface area; P2, middle scallops of posterior mitral leaflet.

multiplanar reconstruction capabilities, and rapid turnaround time (Ranganath et al., 2020).

Today, in addition to surgical interventions, we are seeing a rapid increase in the performance of less invasive transcatheter methods of mitral insufficiency treatment (Wojakowski et al., 2021). Computed tomography is essential for the multiple aspects of planning and performing procedures within the mitral valve, thus avoiding complications. Nevertheless, the multiplanar complexity of the mitral valve apparatus hinders valve assessment in standard tomography reconstructions. It is still a challenge for clinicians to routinely evaluate the mitral valve in detail using computed tomography scans (Kim et al., 2017). A very promising tool that may support this process is semi-automatic image segmentation, which creates three-dimensional (3D) reconstructions of the heart chambers and vessels using computed tomography images. In this study, we sought to compare the morphometrical features of non-diseased mitral valves imaged in cardiac computed tomography with those analyzed macroscopically in autopsied healthy human hearts.

## 2 | MATERIALS AND METHODS

This study was approved by the Bioethical Committee of the Jagiellonian University, Cracow, Poland (No 1072.6120.179.2020). The study protocol conforms to the ethical guidelines of the 1975 Declaration of Helsinki.

### 2.1 | Cardiac computed tomography

In the imaging part of this study, we have analyzed 51 consecutive patients (43.1% males, mean age  $54.6 \pm 14.1$  years old) admitted to the 2nd Department of Cardiology and Cardiovascular Interventions, University Hospital in Krakow, who had performed a cardiac computed tomography. The analysis was specifically performed on patients, whose computed tomography not revealed neither any structural heart disease, valvular disease nor coronary artery disease. None of the 51 patients had a history of any valvular disease in echocardiography as well.

The cardiac computed tomography was performed using a 64-row dual-source scanner (Aquilion 64, Toshiba Medical Systems). The contrast-enhanced electrocardiogram-gated image acquisitions were performed during inspiratory breath hold. The imaging parameters for scanner were a tube voltage of 100–120 kV and an effective tube current of 350–400 mA. The collimation and temporal resolution were  $2 \times 32 \times 0.6 \text{ mm}^3$  and 165 ms, respectively. The arrival time of the contrast agent to the ascending aorta was determined at the level of the trachea bifurcation with the use of a test bolus method (volume of 15 ml of contrast agent, followed by 20 ml of saline). Contrast agent was injected at a dose of 1.0 ml/kg and a rate of 5.5 ml/s followed by 40 ml of saline at the same rate. The acquisition delay was the time of maximum density of the ascending aorta in the test bolus with an additional 6 s of delay. Images were reconstructed with a B26f and B46f kernel and an image matrix of  $512 \times 512$  pixels. Multiphase

reconstruction (from 10 to 100%) was performed and 70% (left ventricle end-diastole) image reconstruction was evaluated. The initial post-processing and study evaluations were performed with the use of multiplanar reconstructions. The 3D reconstruction and visualization software (Mimics Innovation Suite 22, Materialise) was used for heart chambers semi-automatic segmentation (blood pool) and myocardial manual segmentation (tissue segmentation) to visualize a 3D structure of the mitral valve complex and to perform all measurements.

### 2.2 | Autopsied material

The second part of the study was conducted at the Department of Anatomy of the Jagiellonian University Medical College in Cracow, Poland. A total of 120 adult autopsied human hearts (59.2% males), with a mean age of  $50.4 \pm 16.6$  years were investigated. Samples were collected during routine forensic medical autopsies due to incidental deaths at the Department of Forensic Medicine, Jagiellonian University Medical College, Krakow, Poland. We collected data regarding a donor's sex, age, body weight, and height. The exclusion criteria included severe cardiac anatomical defects, heart surgeries or heart grafts, evident severe macroscopic pathologies of the heart or vascular system found during autopsy (aneurysms, storage diseases), heart trauma, history of valvular disease, macroscopic signs of cadaver decomposition. All of the hearts were fixed in a 10% formalin solution for a maximum of 2 months until the time of measurement. Then the left atrium was opened in a routine way and the mitral annulus and mitral valve leaflets were assessed.

### 2.3 | Measurements

To assess mitral valve morphometry the following measurements were performed (Figures 1 and 2):

- mitral annulus diameters: aorto-mural diameter and intercommisural diameter,
- the height of the middle scallops of posterior mitral leaflet (P2) (the distance from the mitral annulus to the free edge of P2, measured in the central part of the base),
- the height of the anterior mitral leaflet (the distance from the mitral annulus to the free edge of anterior mitral leaflet, measured in the central part of the base),
- perimeter of the mitral valve annulus,
- aorto-mural annulus diameter/anterior leaflet ratio,
- intercommisural/aorto-mural diameter ratio.

In computed tomography reconstructions, the linear measurements were taken using virtual calipers in end-diastolic phase. Macroscopic measurements on autopsied material were performed using 0.03 mm precision electronic calipers (YT-7201, YATO). All measurements were performed by two independent investigators and the mean of two values was calculated and reported as a final value.

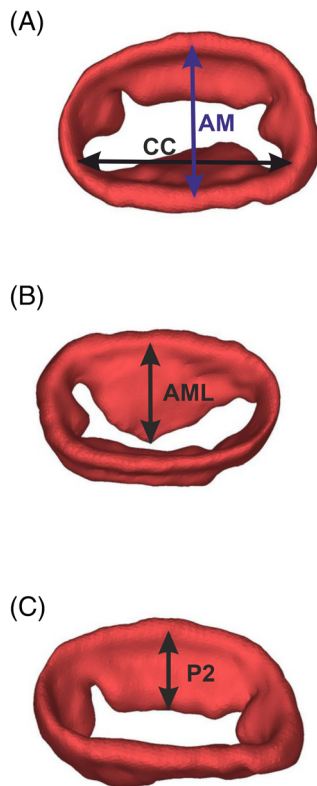


**FIGURE 1** Mitral valve three-dimensional (3D) reconstructions (end-diastole) segmented from contrast enhanced computed tomography of the heart with marked measured dimensions (Mimics Innovation Suite 22, Materialise): (A) Left atrial view of the mitral valve with marked intercommisural (CC) and aorto-mural (AM) diameters. (B) Height of the anterior mitral leaflet (AML). (C) Height of the middle scallops of posterior mitral leaflet (P2).

## 2.4 | Statistical analysis

Continuous variables were presented as mean values with their corresponding standard deviations (SD). Categorical results were presented as numbers and percentages. The normality of the data was assessed with the Shapiro-Wilk test. Student's *t* test and Mann-Whitney test were used for statistical comparisons. Correlation coefficients were calculated to assess whether there was a statistical dependence between the measured parameters. We performed statistical analyses with STATISTICA v13.3 (StatSoft Inc.). The statistical significance was set at a *p*-value lower than 0.05.

## 3 | RESULTS

### 3.1 | Computed tomography

The image quality of computed tomography scans was very good and allows for semi-automatic and manual segmentation and conducting all measurements. In computed tomography group 7 (13.7%) patients suffered from diabetes mellitus, 29 (56.9%) from

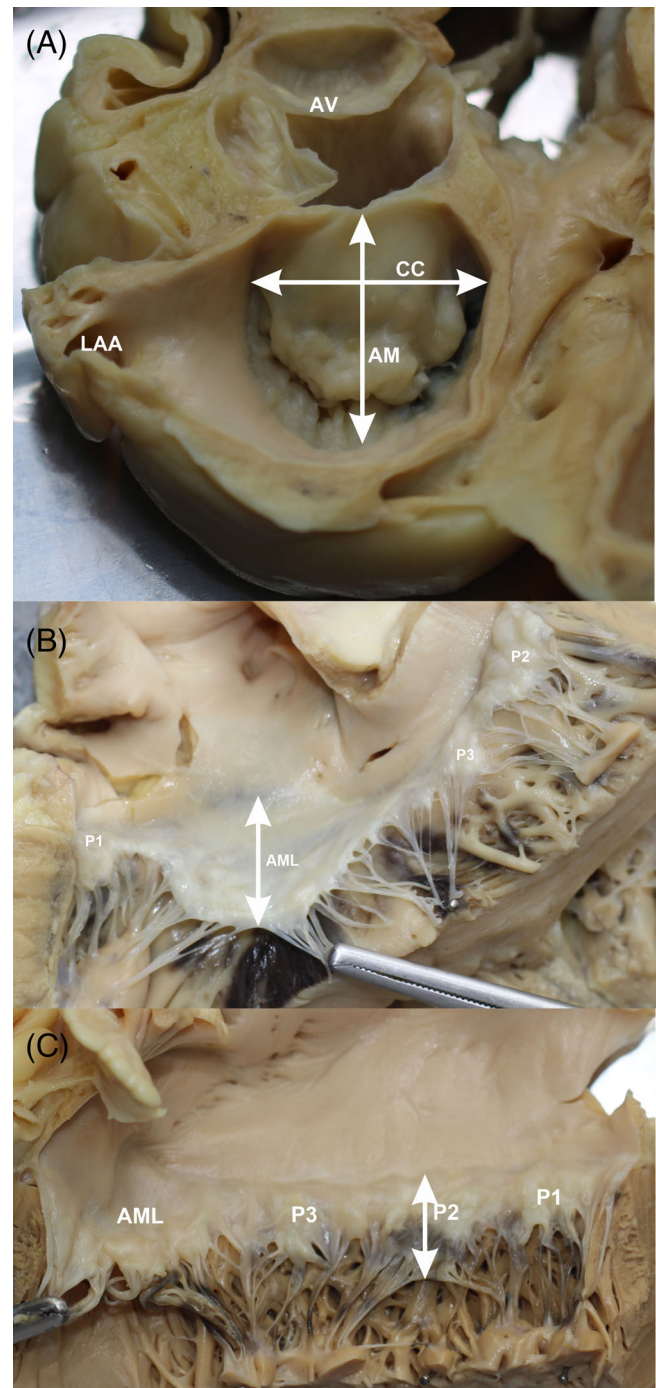


**FIGURE 2** Photographs showing cadaveric heart specimen. (A) Left atrial view of the mitral valve with marked intercommisural (CC) and aorto-mural (AM) diameters. (B) Height of the anterior mitral leaflet (AML) and (C) middle scallops of posterior mitral leaflet (P2). AV, aortic valve; LAA, left atrial appendage; P1, P2, P3, scallops of the posterior mitral leaflet.

hypertension, 1 (2.0%) from chronic obstructive pulmonary disease. Two (3.9%) patients had paroxysmal atrial fibrillation, 14 (27.5%) were active smokers or have recently quit. There was no patient with previous myocardial infarction; stroke and no one had pacemaker or other heart device. The group characteristics and

**TABLE 1** Comparison of group characteristics and corresponding mitral valve parameters measured in autopsied material and cardiac computed tomography (mean  $\pm$  SD).

| Parameter                                   | Autopsied material (N = 120) | Cardiac computed tomography (N = 51) | p-value  |
|---|------------------------------|--------------------------------------|----------|
| Sex (% females)                             | 49 (40.8)                    | 29 (56.9)                            | 0.054    |
| Age (years)                                 | 50.4 $\pm$ 16.6              | 54.6 $\pm$ 14.1                      | 0.116    |
| BMI (kg/m <sup>2</sup> )                    | 26.8 $\pm$ 4.4               | 28.3 $\pm$ 4.7                       | 0.055    |
| BSA (m <sup>2</sup> )                       | 1.91 $\pm$ 0.2               | 1.96 $\pm$ 0.2                       | 0.630    |
| Aorto-mural diameter (mm)                   | 20.2 $\pm$ 4.7               | 26.1 $\pm$ 3.6                       | < 0.0001 |
| Intercommissural diameter (mm)              | 28.2 $\pm$ 4.8               | 36.2 $\pm$ 5.6                       | < 0.0001 |
| Intercommissural/aorto-mural diameter ratio | 1.5 $\pm$ 0.4                | 1.4 $\pm$ 0.2                        | 0.259    |
| Perimeter of the mitral valve annulus (mm)  | 89.8 $\pm$ 12.1              | 98.7 $\pm$ 12.6                      | < 0.0001 |
| Height of the P2 (mm)                       | 13.0 $\pm$ 2.9               | 13.1 $\pm$ 2.5                       | 0.264    |
| Height of the AML (mm)                      | 20.7 $\pm$ 4.1               | 18.3 $\pm$ 3.8                       | 0.0007   |
| Aorto-mural annulus/anterior leaflet ratio  | 1.0 $\pm$ 0.3                | 1.6 $\pm$ 0.3                        | < 0.0001 |

Abbreviations: AML, anterior mitral leaflet; BMI, body mass index; BSA, body surface area; N, number; P2, middle scallops of posterior mitral valve leaflet.

measured parameters are reported in Table 1. In all investigated cases, the intercommissural mitral valve diameter was bigger than the aorto-mural diameter (36.2  $\pm$  5.6 vs. 26.1  $\pm$  3.6 mm;  $p < 0.0001$ ). Some differences between sexes were found in cardiac computed tomography measurements. Larger dimensions were observed in males compared to females: intercommissural mitral diameter (39.9  $\pm$  5.1 vs. 33.5  $\pm$  4.3 mm;  $p = 0.0001$ ), aorto-mural diameter (27.5  $\pm$  2.5 vs. 24.9  $\pm$  4.0 mm;  $p = 0.010$ ), perimeter of the mitral valve annulus (107.0  $\pm$  9.5 vs. 92.4  $\pm$  11.0 mm;  $p < 0.0001$ ) and the height of the P2 scallop (14.4  $\pm$  1.9 vs. 12.2  $\pm$  2.5 mm;  $p = 0.002$ ). Significant correlations between the body surface area (BSA) and all measured parameters were found in computed tomography: aorto-mural diameter ( $r = 0.35$ ,  $p = 0.016$ ), intercommissural diameter ( $r = 0.51$ ,  $p < 0.001$ ), the height of P2 scallop ( $r = 0.50$ ,  $p < 0.001$ ), the height of the anterior mitral leaflet ( $r = 0.30$ ,  $p = 0.041$ ) and perimeter ( $r = 0.57$ ,  $p < 0.001$ ). Additionally, there were correlations between the body mass index (BMI) and aorto-mural diameter ( $r = 0.38$ ,  $p = 0.010$ ), BMI and the height of P2 scallop ( $r = 0.31$ ,  $p = 0.036$ ), between age and both mitral valve diameters (aorto-mural:  $r = -0.479$ ,  $p = 0.001$ ; intercommissural:  $r = -0.433$ ,  $p = 0.003$ ), age and perimeter of the mitral annulus ( $r = -0.517$ ,  $p < 0.001$ ), age and the height of the P2 ( $r = -0.304$ ,  $p = 0.040$ ).

### 3.2 | Autopsied material

All of 120 human hearts had classical mitral valve type. The group characteristics and measured parameters are reported in Table 1. The intercommissural mitral valve diameter was larger than the aorto-mural diameter (28.2  $\pm$  4.8 vs. 20.2  $\pm$  4.7 mm;  $p < 0.0001$ ). Significant differences between sexes were found such as larger intercommissural mitral diameter (13.4  $\pm$  3.0 vs. 11.8  $\pm$  2.3 mm;  $p = 0.002$ ) and larger height of the P2 scallop (28.8  $\pm$  4.8 vs. 26.7  $\pm$  4.7 mm;  $p = 0.018$ ) in males compared to females.

In autopsied group some significant correlations between the BSA and the height of P2 scallop ( $r = 0.23$ ,  $p = 0.011$ ) and the height of the anterior mitral leaflet ( $r = 0.19$ ,  $p = 0.041$ ) were found. Additionally, there were correlations between the age and aorto-mural diameter ( $r = 0.33$ ,  $p = 0.0002$ ). There were no other notable correlations found between parameters and anthropometric features of donors.

### 3.3 | Groups comparison

Both the imaging and autopsied study groups were comparable in terms of anthropometric characteristic of patients/donors (Table 1). Direct comparison of corresponding mitral valve parameters revealed significant differences between obtained results (Table 1). Significantly larger intercommissural diameter, aorto-mural diameter, and perimeter of the mitral annulus were observed in tomographic scans (Table 1, all  $p < 0.0001$ ). However, the intercommissural/aorto-mural diameter ratio showed comparable values for both groups. Nevertheless, the size of anterior mitral leaflet was higher in autopsied material (Table 1,  $p = 0.001$ ). The height of the P2 scallops was the only parameter that show no significant difference between two groups ( $p = 0.3$ ).

## 4 | DISCUSSION

The mitral valve apparatus consists of the annulus, along with two leaflets, two commissures, two groups of papillary muscles, tendinous cords, and parts of the left ventricular and atrial walls (Krawczyk-Ożóg, Hołda, Bolechała, et al., 2017; Krawczyk-Ożóg, Hołda, Sorysz, et al., 2017). Imaging in computed tomography, especially with the implementation of modifications to the acquisition protocol and post-processing workup, allows for the assessment of all components of the mitral apparatus. In this article, we show 3D reconstructions of

the mitral valve annulus and leaflets and compare their measurements with autopsied materials. Besides facilitating the taking of measurements and observations, the additional benefits of 3D imaging include the ability to show in detail the individual components of the valve, especially the commissures, the connection of the scallops and additional scallops which are common in mitral valves (Krawczyk-Ożóg, Hołda, Sorysz, et al., 2017) (Figure 1). Moreover, computed tomography is also sensitive to the detection of annular calcification and leaflet degeneration (Blanke et al., 2014).

We have also observed rapid development of minimally invasive medicine where transcatheter procedures have provided feasible and safe alternatives to medical and surgical treatment, especially for patients who are not considered suitable candidates for conventional mitral valve surgery (De Backer et al., 2021). Better imaging techniques could help with patient selection, choice of treatment method, preprocedural sizing, and improved clinical outcomes. All technologies that are based on the percutaneous reshaping of the mitral annulus (direct or indirect annuloplasty), as well as transcatheter mitral valve implantation need a preprocedural assessment of the mitral annulus anatomy for guiding patient selection and for planning the procedure (Gordic et al., 2014; Patterson et al., 2019; Wojakowski et al., 2021). Therefore, the assessment of mitral annular dimensions by cross-sectional imaging such as computed tomography is of increasing relevance (Blanke et al., 2014).

The mitral annulus is a nonsymmetric, nonplanar fibrous structure with a 3D saddle-shaped configuration (Weir-McCall et al., 2018). To evaluate its size, we measured both its dimensions and perimeter, which were larger in computed tomography compared to the autopsied material. It should be emphasized, that both the dimensions of the cadaveric mitral valve components and those obtained using imaging techniques may differ from those that are present *in vivo*. Moreover, the mitral valve annulus has a dynamic geometry that changes in the cardiac cycle, which unfortunately cannot be assessed in computed tomography or during autopsy. The opposite differences in size were found in the anterior mitral leaflet height, which was considerably larger in the autopsied material. This may be due to the greater accuracy of the macroscopic measurement of the tissue. Measurements of the cadaveric heart allow for examination of the unfold leaflet with a well-marked attachment line and a free edge of the leaflet that, due to its low thickness, may be blurred in computed tomography examination.

Previous studies evaluating the mitral valve annulus in patients with no evident cardiac disease revealed a perimeter between 9.3 and 12.3 cm. The mean value of the mitral annulus in healthy humans was 9.3 cm using in a 2D transthoracic echocardiography measured in diastole and 11.4 cm using 3D transesophageal echocardiography measured in systole (Khabbaz et al., 2013; Levine et al., 1989; Ormiston et al., 1981). The mean value of the mitral annulus was 11.6 cm when using a 3D approach with magnetic resonance imaging in diastole (Maffessanti et al., 2013). In computed tomography (measured in diastole), the values for the mitral valve perimeter in two- and 3D modality were 11.8 and 12.3 cm, respectively (Gordic et al., 2014). All the above methods overestimated the

measurements compared to the autopsy material analyzed in our population of 120 hearts, where the mean value of the perimeter was  $8.9 \pm 1.2$  cm. On the other hand, the mean perimeter annulus obtained in computed tomography after 3D segmentation ( $9.9 \pm 1.3$  cm) was closer to the autopsied material and 2D echocardiography than in other tomographic studies (Gordic et al., 2014; Naoum et al., 2016). When comparing two- versus three-dimensional measurements in cardiac computed tomography, a significant difference for all circumference measurements may be found. A systematic underestimation of the posterior circumference for a 2D evaluation (ranging between 1.8 and 2.1 mm) is present in normal cases and patients with functional mitral regurgitation. This further highlights the 3D nature of the mitral annulus (Gordic et al., 2014).

An aorto-mural diameter of the mitral annulus greater than 35 mm or an aorto-mural annulus/anterior leaflet ratio greater than 1.3 are considered indicators of mitral annular dilatation (Caldarera et al., 1995; Lancellotti et al., 2013; Sorysz et al., 2020). Our analysis of autopsied structurally unchanged showed lower values for both parameters, indicating the correctness of these parameters. However, in computer tomography, the aorto-mural annulus/anterior leaflet ratio was significantly higher ( $1.6 \pm 0.3$ ), what should be taken into account when interpreting the results of tomography. This difference was a result of the smaller size of the anterior mitral leaflet measured in computed tomography.

Certain study limitations must be acknowledged. It is a single center study with a relatively small-sized computed tomography study group. The 3D segmentation tool (Mimics Innovation Suite 22, Materialise) used is not a standard clinical instrument utilized in everyday clinical practice, and its availability is low. Moreover, there is a potential bias in the measurements of autopsied materials because all of the hearts were preserved in formaldehyde, which may slightly change the size and shape of the heart. Although prior studies have shown that the dimensions of hearts preserved in 10% paraformaldehyde solution are similar to those before fixation (Hołda et al., 2016), the summation of inaccuracies resulting from two different measurement groups and techniques (tissue preservation, rigor mortis, image acquisition, image post processing, cardiac cycle) may be responsible for the observed differences in results. However, we believe that these limitations did not impede our morphologic analysis or the conclusions drawn.

## 5 | CONCLUSION

The use of 3D postprocessing algorithms provides a very accurate image of the mitral valve structure, which could be useful for the precise non-invasive assessment of mitral valve size and structure. Our study provides information on mitral annulus dimensions, including both diameters, perimeter and leaflet height, measured in both 3D computed tomography and autopsied material that may be used as reference data for a healthy population. Contrast enhanced cardiac computed tomography significantly overestimates the measurements of the mitral annulus compared to postmortem analysis.

## ACKNOWLEDGMENTS

The authors sincerely thank those who donated their bodies to science so that anatomical research could be performed. Results from such research can potentially increase mankind's overall knowledge that can then improve patient care. Therefore, these donors and their families deserve our highest gratitude.

## ORCID

Agata Krawczyk-Ożóg  <https://orcid.org/0000-0001-7691-8174>

Mateusz K. Hołda  <https://orcid.org/0000-0001-5754-594X>

Jakub Batko  <https://orcid.org/0000-0002-5329-5856>

Stanisław Bartuś  <https://orcid.org/0000-0003-4508-3551>

## REFERENCES

- Blanke, P., Dvir, D., Cheung, A., Ye, J., Levine, R. A., Precious, B., Berger, A., Stub, D., Hague, C., Murphy, D., Thompson, C., Munt, B., Moss, R., Boone, R., Wood, D., Pache, G., Webb, J., & Leipsic, J. (2014). A simplified D-shaped model of the mitral annulus to facilitate CT-based sizing before transcatheter mitral valve implantation. *Journal of Cardiovascular Computed Tomography*, 8(6), 459–467. <https://doi.org/10.1016/J.JCCT.2014.09.009>
- Caldarera, I., Herwerden, L. V., Taams, M. A., Bos, E., & Roelandt, J. R. T. C. (1995). Multiplane transoesophageal echocardiography and morphology of regurgitant mitral valves in surgical repair. *European Heart Journal*, 16(7), 999–1006. <https://doi.org/10.1093/oxfordjournals.eurheartj.a061037>
- De Backer, O., Wong, I., Taramasso, M., Maisano, F., Franzen, O., & Søndergaard, L. (2021). Transcatheter mitral valve repair: An overview of current and future devices. *Open Heart*, 8(1), e001564. <https://doi.org/10.1136/OPENHRT-2020-001564>
- Douedi, S., & Douedi, H. (2021). *Mitral regurgitation*. StatPearls Publishing. <https://www.ncbi.nlm.nih.gov/books/NBK553135/> 9 February 2022.
- Gordic, S., Nguyen-Kim, T. D. L., Manka, R., Sündermann, S., Frauenfelder, T., Maisano, F., Falk, V., & Alkadhi, H. (2014). Sizing the mitral annulus in healthy subjects and patients with mitral regurgitation: 2D versus 3D measurements from cardiac CT. *International Journal of Cardiovascular Imaging*, 30(2), 389–398. <https://doi.org/10.1007/s10554-013-0341-4>
- Hołda, M. K., Klimek-Piotrowska, W., Koziej, M., Piątek, K., & Hołda, J. (2016). Influence of different fixation protocols on the preservation and dimensions of cardiac tissue. *Journal of Anatomy*, 229(2), 334–340. <https://doi.org/10.1111/JOA.12469>
- Khabbaz, K. R., Mahmood, F., Shakil, O., Warrach, H. J., Gorman, J. H. 3rd, Gorman, R. C., Matyal, R., Panzica, P., & Hess, P. E. (2013). Dynamic three-dimensional echocardiographic assessment of mitral annular geometry in patients with functional mitral regurgitation. *The Annals of Thoracic Surgery*, 95(1), 105–110. <https://doi.org/10.1016/J.ATHORACSUR.2012.08.078>
- Kim, J. H., Kim, E. Y., Jin, G. Y., & Choi, J. B. (2017). A review of the use of cardiac computed tomography for evaluating the mitral valve before and after mitral valve repair. *Korean Journal of Radiology*, 18(5), 773–785. <https://doi.org/10.3348/kjr.2017.18.5.773>
- Krawczyk-Ożóg, A., Hołda, M. K., Bolechała, F., Siudak, Z., Sorysz, D., Dudek, D., & Klimek-Piotrowska, W. (2017). Anatomy of the mitral sub-valvular apparatus. *The Journal of Thoracic and Cardiovascular Surgery*, 155, 2002–2010. <https://doi.org/10.1016/j.jtcvs.2017.12.061>
- Krawczyk-Ożóg, A., Hołda, M. K., Sorysz, D., Koziej, M., Siudak, Z., Dudek, D., & Klimek-Piotrowska, W. (2017). Morphologic variability of the mitral valve leaflets. *The Journal of Thoracic and Cardiovascular Surgery*, 154(6), 1927–1935. <https://doi.org/10.1016/J.JTCVS.2017.07.067>
- Lancellotti, P., Tribouilloy, C., Hagendorff, A., Popescu, B. A., Edvardsen, T., Pierard, L. A., Badano, L., & Zamorano, J. L. (2013). Recommendations for the echocardiographic assessment of native valvular regurgitation: An executive summary from the European Association of Cardiovascular Imaging. *European Heart Journal Cardiovascular Imaging*, 14(7), 611–644. <https://doi.org/10.1093/ehjci/jet105>
- Levine, R. A., Handschumacher, M. D., Sanfilippo, A. J., Hagege, A. A., Harrigan, P., Marshall, J. E., & Weyman, A. E. (1989). Three-dimensional echocardiographic reconstruction of the mitral valve, with implications for the diagnosis of mitral valve prolapse. *Circulation*, 80(3), 589–598. <https://doi.org/10.1161/01.CIR.80.3.589>
- Maffessanti, F., Gripari, P., Pontone, G., Andreini, D., Bertella, E., Mushtaq, S., Tamborini, G., Fusini, L., Pepi, M., & Caiani, E. G. (2013). Three-dimensional dynamic assessment of tricuspid and mitral annuli using cardiovascular magnetic resonance. *European Heart Journal - Cardiovascular Imaging*, 14(10), 986–995. <https://doi.org/10.1093/EHJCI/JET004>
- Naoum, C., Leipsic, J., Cheung, A., Ye, J., Bilbey, N., Mak, G., Berger, A., Dvir, D., Arepalli, C., Grewal, J., Muller, D., Murphy, D., Hague, C., Piazza, N., Webb, J., & Blanke, P. (2016). Mitral annular dimensions and geometry in patients with functional mitral regurgitation and mitral valve prolapse implications for transcatheter mitral valve implantation. *JACC: Cardiovascular Imaging*, 9(3), 269–280. <https://doi.org/10.1016/j.jcmg.2015.08.022>
- Ormiston, J. A., Shah, P. M., Tei, C., & Wong, M. (1981). Size and motion of the mitral valve annulus in man. I. A two-dimensional echocardiographic method and findings in normal subjects. *Circulation*, 64(1), 113–120. <https://doi.org/10.1161/01.CIR.64.1.113>
- Patterson, T., Adams, H., Allen, C., Rajani, R., Prendergast, B., & Redwood, S. (2019). Indirect annuloplasty to treat functional mitral regurgitation: Current results and future perspectives. *Frontiers in Cardiovascular Medicine*, 6, 60. <https://doi.org/10.3389/FCVM.2019.00060>
- Ranganath, P., Moore, A., Guerrero, M., Collins, J., Foley, T., Williamson, E., & Rajiah, P. (2020). CT for pre-and postprocedural evaluation of transcatheter mitral valve replacement. *Radiographics*, 40(6), 1528–1553. <https://doi.org/10.1148/rg.2020200027>
- Sorysz, D., Krawczyk-Ożóg, A., Dziewierz, A., Tokarek, T., Zawiaślak, B., Hołda, M., Komnata, K., Surdacki, A., Bartuś, S., & Dudek, D. (2020). Assessment of mitral regurgitation and mitral complex geometry in patients after transcatheter aortic valve implantation. *Advances in Interventional Cardiology/Postępy w Kardiologii Interwencyjnej*, 16(3), 300–305. <https://doi.org/10.5114/AIC.2020.99265>
- Weir-McCall, J. R., Blanke, P., Naoum, C., Delgado, V., Bax, J. J., & Leipsic, J. (2018). Mitral valve imaging with CT: Relationship with transcatheter mitral valve interventions. *Radiology*, 288(3), 638–655. <https://doi.org/10.1148/RADIOL.2018172758/ASSET/IMAGES/LARGE/RADIOL.2018172758.TBL2.JPEG>
- Wojakowski, W., Chmielak, Z., Widenka, K., Pręgowski, J., Perek, B., Gackowski, A., Bartuś, K., Szymański, P., Deja, M. A., Kalarus, Z., Suwalski, P., Trębacz, J., Kołsut, P., Ścisło, P., Wróbel, K., Smolka, G., Gerber, W., Dudek, D., Hirmler, T., ... Kuśmierczyk, M. (2021). Transcatheter mitral valve repair and replacement. Expert consensus statement of the Polish Cardiac Society and the Polish Society of Cardiothoracic Surgeons. *Kardiologia Polska (Polish Heart Journal)*, 79(10), 1165–1177. <https://doi.org/10.33963/KP.A2021.0116>

**How to cite this article:** Krawczyk-Ożóg, A., Hołda, M. K., Batko, J., Bartuś, S., & Rajtar-Salwa, R. (2023). Three-dimensional cardiac computed tomography compared with autopsied material for the assessment of the mitral valve. *Clinical Anatomy*, 36(2), 250–255. <https://doi.org/10.1002/ca.23967>